Table II. Some Estimated $\Delta_f H°(CH_3X)$ (kcal mol^{-1})

X	V_X	$\Delta_f H°(HX)^a$	p	$\Delta_f H°(CH_3X)_{est}$
GeH_3	3.24	21.7	4	4.4 ± 2.0
SnH_3	2.83	38.9	4	18.6 ± 2.0
PH_2	4.55	1.3	3	-4.6 ± 1.5
AsH_2	4.20	15.9	3	8.1 ± 1.5
SeH	5.13	7.1	2	5.3 ± 1.0

[a] Reference 10.

Polyvalent Atoms, X

For polyvalent atoms X, a similar straight line has been found, as shown by line I in Figure 2. The equation for line II is given by

$$\Delta\Delta_f H°(CH_3X/HX)/p = -10.2 + 1.81V_X \quad (3)$$

where X = OH, SH, NH_2, CH_3, and SiH_3. The average and maximum deviations from line II are also only 0.3 and 0.5 kcal per hydrogen atom in HX, respectively. It is interesting to note that the groups X = OH, NH_2, and SH fall equally close to lines I or II. Only X = CH_3 and SiH_3 fall uniquely on line II. Since the two lines are very close to each other it is possible to represent all the data by a single, mean linear relation having larger deviations. The maximum deviation is about 2 kcal per hydrogen atom in HX. This cruder linear equation is given by

$$\Delta\Delta_f H°(CH_3X/HX)/p = -13.6 + 2.30V_X \quad (4)$$

In general, we have a relatively precise linear equation for the two categories:

$$\Delta\Delta_f H°(CH_3X/HX)/p = a' + b'V_X \quad (5)$$

Discussion

Empirical eq 5 can be used for estimating heats of formation of some compounds, CH_3X or HX. For example, we have derived from eq 3

$$\Delta_f H°(CH_3X)_{est} = (-10.2 + 1.81V_X)p + \Delta_f H°(HX) \quad (6)$$

Using known data for $\Delta_f H°(HX)$, where X = GeH_3, SnH_3, PH_2, AsH_2, and SeH, we can estimate $\Delta_f H°(CH_3X)$ (see Table II). The heats of formation of these CH_3X have not yet been measured.

Combining eq 1 with 5, we have a new linear equation

$$\Delta\Delta_f H°(RX/HX) = (a_m + a'p) + (b_m + b'p)V_X \quad (7)$$

If X is a polyvalent atom, then

$$\Delta\Delta_f H°(RX/HX) = [0.9 - 1.5m(m-1) - 10.2p] + \left[1.81p - \frac{m}{0.67 + 0.21m}\right]V_X \quad (8)$$

or

$$\Delta_f H°(RX)_{est} = [0.9 - 1.5m(m-1) - 10.2p] + \left[1.81p - \frac{m}{0.67 + 0.21m}\right]V_X + \Delta_f H°(HX) \quad (9)$$

Equation 9 can be used for estimating heats of formation of many kinds of compounds, such as $CH_3CH_2SiH_3$, $(CH_3)_2CHGeH_3$, $(CH_3)_3CPH_2$, $(CH_3)_2CHAsH_2$, and C_2H_5SeH.

Thermochemists have sought for a long time to find methods for the quantitative estimation of the heats of formation of chemical compounds from carefully measured data on "key" members of homologous series. The need for and the utility of such methods are well documented.[6,11,12] With the discovery of V_X as a measure of the electronegativity and its successful application to differences in heats of formation we seem to have found such a method. We are currently exploring its application to a variety of other elements and properties such as ionization potentials where it again seems to produce remarkably quantitative correlations. We hope to report on these efforts in the near future. We shall also in these papers compare some of the results found by using other electronegativity scales.

$V_X = n_X/r_X$ is proportional to the (nucleus-core) potential, $e^2[Z - (Z - n_X)]/r_X$, experienced by a bonding electron at the covalent binding distance. it seems intuitively plausible that the strength of a covalent bond would show a dependence on V_X. It also seems reasonable that there will be a compensating potential in an actual compound due to the other bonding electrons, the nuclei to which they are attached, and their distances from the bond being considered. These latter influences might account in part for the appearance of p and m in our relationships.

Acknowledgment. This work has been supported by grants from The National Science Foundation (CHE-8714647) and The U.S. Army Research Office (DAAG29-85-K-0019).

(11) Benson, S. W. *Thermochemical Kinetics*, 2nd ed.; Wiley: New York, 1976.
(12) Cox, J. D.; Pilcher, G. *Thermochemistry of Organic and Organometallic Compounds*; Academic Press: New York, 1970.
(13) Huber, K. P.; Herzberg, G. *Molecular Spectra and Molecular Structure, IV, Constants of Diatomic Molecules*; VNR Co.: New York, 1979.
(14) Pauling, L. *J. Am. Chem. Soc.* **1947**, *69*, 542.
(15) Little, E. J., Jr.; Jones, M. M. *J. Chem. Educ.* **1960**, *37*, 231.

On the Electrostatic Bonding of CO to the Monocations of the First-Row Transition Elements

A. Mavridis,[†] J. F. Harrison,* and J. Allison

Contribution from the Department of Chemistry, Michigan State University, East Lansing, Michigan 48824-1322. *Received May 9, 1988*

Abstract: We have investigated the binding of a CO group to the early transition metal +1 ions Sc^+, Ti^+, V^+, and Cr^+ using ab initio electronic structure theory and find that the binding mechanism is electrostatic in nature with no more than 10% σ ligand-to-metal donations and practically no metal-to-ligand π donation. Our calculated M–C^+ bond lengths are very long, ranging from 2.25 Å in $CrCO^+$ ($^4\Pi$) to 3.38 Å in $ScCO^+$ ($^3\Sigma^+$). The calculated binding energies range from 3.4 kcal/mol in the $^3\Sigma^+$ state of $ScCO^+$ to 21.5 kcal/mol in the $^4\Pi$ state of $CrCO^+$ and correlate with the equilibrium M–C distance.

A well-known aspect of the first-row transition metal elements is their ability to form complexes with neutral ligands, most notably the carbonyl ligand,[1,2] CO. The mechanism through which carbon monoxide binds to neutral or (formally) low oxidation states of transition metal elements is of fundamental interest in organometallic chemistry.

[†] On leave from the Department of Chemistry, University of Athens, Greece.

(1) Cotton, F. A.; Wilkinson, G. *Advanced Inorganic Chemistry*; John Wiley: New York, 1980.
(2) See, for example: Klein, K. *Adv. Catal.* **1982**, *31*, 243. Dekleva, T. W.; Foster, *Ibid.* **1986**, *34*, 81.

0002-7863/89/1511-2482$01.50/0

Table I. Total Molecular Energies, Equilibrium Bond Lengths, and Bond Energies for Various $ScCO^+$, $TiCO^+$, VCO^+, and $CrCO^+$ Electronic States[a]

molecule	state	energy (hartrees)	R(M–C) (Å)	D_e (kcal mol^{-1})	asymptotic M^+ products (CO always in $X^1\Sigma^+$)
$ScCO^+$	$^3\Delta$ ($^3A_2$)	−872.386 30	2.739	9.1	^3D
	$^3\Delta$ (CI, 36 039 CSF's)[b]	−872.514 90	1.697	10.2	^3D
	$^3\Pi$ ($^3B_1$)	−872.383 49	2.755	7.3	^3D
	$^3\Sigma^+$ ($^3A_1$)	−872.377 21	3.385	3.4	^3D
	$^3\Sigma^-$ ($^3A_2$)	−872.351 07	2.471	13.5	$^3F + {}^3P$
$TiCO^+$	$^4\Sigma^-$ ($^4A_2(sd^2)$)	−961.034 85	2.633	8.7	$2/\sqrt{5}\|^4F\rangle - 1/\sqrt{5}\|^4P\rangle$
	$^4\Sigma^-$ (CI, 54 429 CSF's)[b]	−961.191 41	2.663	7.2	
	$^4\Sigma^-$ ($^4A_2$ (d^3))	−961.035 12	2.498	8.9	
VCO^+	$^5\Delta$ ($^5A_1$)	−1055.520 52	2.489	11.4	^5F
	$^5\Delta$ (CI, 73 787 CSF's)[b]	−1055.677 02	2.504	10.0	^5D
$CrCO$	$^6\Sigma^+$ ($^6A_1$)	−1155.978 51	2.479	13.5	^6S
	$^6\Sigma^+$ (CI, 66 338 CSF's)[b]	−1156.175 74	2.335	13.9	^6S
	$^4\Sigma$ ($^4B_2$)	−1155.850 72	2.250	21.5	$C_1\|^4G\rangle + C_2\|^4P\rangle + C_3\|^4D\rangle$[c]

[a] Results refer to GVB (4/8) calculations except where noted; the SCF energies for Sc^+, Ti^+, V^+, and Cr^+ are reported in Table I of ref 24. [b] CI's are of SCF+1+2 type using the GVB correlated orbitals; numbers in parentheses indicate the number of configuration state functions included in the CI's. [c] This "contaminated" state comes from the $d^0_\sigma d^2_{\pi_y} d^1_{\pi_x} d^1_{\Delta_+} d^1_{\Delta_-}$ electron distribution on Cr^+.

The binding mechanism of CO to transition metals has often been approached within the framework of the traditional Dewar–Chatt[1,3] scheme, which involves ligand-to-metal σ donation with concomitant metal-to-ligand d_π back-donation ("back-bonding"). Although early ab initio descriptions supported this picture,[4] more recent calculations suggest a modified version of the traditional view.[5,6] In particular, the bonding contribution of the σ CO donation to *neutral* metal atoms such as Cu, Ni, and Fe is far less important than the d_π back-donation to the available $2\pi^*$ orbitals of the ligand.

We present calculations of the early transition metal cations, $M^+ = Sc^+$, Ti^+, V^+, and Cr^+, interacting with a single carbonyl molecule forming MCO^+. Our results indicate that, in this instance, a bonding mechanism other than Dewar–Chatt is operative. We find that the M^+–CO interaction is, in essence, *electrostatic* in nature.[7] The large orbital angular momentum of the transition metal ion results in many low-lying electronic states in the MCO^+ molecule. The selection of states studies is representative rather than complete. In all states examined we find little σ donation and practically no d_π back-donation. Similar results were reported recently for the molecules $NiCO^+$[8] and $CuCO^+$.[9]

Computational Details

The basis set for all metals is Wachters[10] 14s9p5d basis, augmented with two additional diffuse p functions[11] to represent the 4p orbitals, and an extra d function.[12] The resulting 14s11p6d primitive set was contracted to 5s4p3d according to Raffenetti.[13] The basis set for both C and O is the Duijneveldt[14] 11s7p augmented with additional s and p functions selected in an even-tempered way, and two single-component d functions on C (α_d = 0.60, 0.20) and on O (α_d = 0.80, 0.25). The resulting 12s8p2d basis was contracted to 4s4p2d according to Raffenetti.[13] Occasionally, a smaller basis set for the CO moiety, 11s7p1d contracted to 3s2p1d, was used for exploratory calculations. All computations were performed using the Argonne National Laboratory collection of QUEST-164 codes.

Our basic computational ansatz is a GVB (4/8) wave function[15] for the carbonyl ligand. Four electron pairs are correlated in a valence bond fashion, the four pairs being the lone pair on carbon, those in the σ bond, and those in two π bonds in the C–O molecule. The metal is kept at the SCF level, and our asymptotic wave function for the combined MCO^+ system can be described as follows:

$$\text{(Ar core)}\quad 1\sigma^2 2\sigma^2 3\sigma^2 (4\sigma^2 - \lambda 6\sigma^{*2})(5\sigma^2 - \mu 7\sigma^{*2})\cdot (1\pi_x^2 - \nu 2\pi_x^{*2})\,(1\pi_y^2 - \nu 2\pi_y^{*2}) 4s^i 3d^j \quad (1)$$

where $\lambda, \mu, \nu \geq 0$. If $\lambda = \mu = \nu = 0$, the SCF description is obtained. The notation "Ar core" indicates that the 18 core electrons of the metal ion are always treated at the SCF level. With the CO molecule in its $X^1\Sigma^+$ state, all the ensuing states of the complex MCO^+ arise from the active space ($4s^i 3d^j$) of the metal ion.

The GVB (4/8) wave function describes the electronic distribution of the free CO fairly well, predicting the correct sign of its dipole moment ($C^{\delta-}$–$O^{\delta+}$) with a dipole moment of 0.124 D (the experimental value being 0.1222 D[16]). The experimental bond length of free CO is 2.132 bohrs,[17] while the small basis GVB (4/8) result is 2.156 bohrs. A geometry optimization of the $ScCO^+$ $^3\Sigma^-$ state with the same basis set results in a C–O bond length of 2.153 bohrs. In all subsequent calculations the C–O distance was kept constant at 2.15 bohrs. CI calculations, at the SCF+1+2 level, using the GVB orbitals have been carried out on the ground states of the species examined, and the results are in essential agreement with the more compact GVB (4/8) description (eq 1). Correcting the CI results for unlinked clusters with Davidson's formula[18] improves the binding energies by ~1 kcal mol^{-1}, an indication of the acceptable level of the present calculations. Our reported values in Table I do not include the Davidson correction. Charge migration between the metal cation(s) and the ligand was extracted from the GVB wave functions according to Mulliken.[19] Both basis sets used in the present study produce similar population analysis results.[20]

To investigate the magnitude of the superposition error, the molecule $ScCO^+$ ($^3\Sigma^-$) was studied using the counterpoise technique.[21] The SCF energy of Sc^+ in the presence of the CO orbitals (at the equilibrium geometry of $ScCO^+$) is 0.07 kcal/mol lower than that of free Sc^+ while the SCF energy of CO in the field of Sc^+ in the same geometry is 0.11 kcal/mol lower. We assume that the basis set superposition error (BSE) for $ScCO^+$ is representative of others in this study and that the BSE is about 0.1 kcal/mol which we consider to be negligible.

Results and Discussion

In Table I we report total energies, equilibrium M–C bond lengths as obtained from polynomial fitting of the corresponding potential curves, and dissociation energies (D_e) with respect to the asymptotic products, M^+ and CO ($^1\Sigma^+$). The irreducible representation symbols accompanying the spectroscopic term

(3) Dewar, M. T. S. *Bull. Soc. Chim. Fr.* **1950**, *18*, C71. Chatt, J. *Research* **1951**, *4*, 180. Chatt, J.; Duncanson, L. *J. Chem. Soc.* **1933**, 2939.
(4) Bagus, P. S.; Nelin, C. J.; Bauschlicher, C. W., Jr. *Phys. Rev.* **1983**, *B28*, 5423.
(5) Bauschlicher, C. W., Jr.; Bagus, P. S. *J. Chem. Phys.* **1984**, *81*, 5889.
(6) Bauschlicher, C. W., Jr.; Bagus, P. S.; Nelin, C. J. *J. Chem. Phys.* **1986**, *85*, 354.
(7) Allison, J.; Mavridis, A.; Harrison, J. F. *Polyhedron* **1988**, *7*, 1559.
(8) Bauschlicher, C. W., Jr. *J. Chem. Phys.* **1986**, *84*, 260.
(9) Merchan, M.; Nebot-Gil, I.; Gonzalez-Luque, R.; Orti, E. *J. Chem. Phys.* **1987**, *87*, 1690.
(10) Wachters, A. J. H. *J. Chem. Phys.* **1970**, *52*, 1033.
(11) Dunning, T. J., Jr., private communication.
(12) Hay, P. *J. Chem. Phys.* **1977**, *66*, 4377.
(13) Raffenetti, R. C. *J. Chem. Phys.* **1973**, *58*, 4452.
(14) Duijneveldt, F. B. IBM Research Laboratory, San Jose, CA 1971; IBM Technical Research Report No. RJ-945.
(15) See, for example: Bobrowitz, F. W.; Goddard, W. A., III In *Modern Theoretical Chemistry: Methods of Electronic Structure Theory*; Schaefer, H. F., III, Ed.; Plenum: New York, 1977; Vol. 3.
(16) Muenter, J. S. *J. Mol. Spectrosc.* **1975**, *55*, 490.
(17) Huber, K. P.; Herzberg, G. *Constants of Diatomic Molecules*; Van Nostrand: New York, 1979.
(18) Davidson, E. R. In *The World of Quantum Chemistry*; Daudel, R., Pullman, B., Eds.; Reidel: Dodrecht, Netherlands, 1974. Langhoff, S. R.; Davidson, E. R. *Int. J. Quantum Chem.* **1974**, *8*, 61.
(19) Mulliken, R. S. *J. Chem. Phys.* **1955**, *23*, 1833, 1841, 2338, 2343. For a critique, see: Noel, J. O. *Inorg. Chem.* **1982**, *21*, 11.
(20) Mulliken, R. S.; Emler, W. C. *Diatomic Molecules*; Academic Press: New York, 1977; pp 33–38.
(21) Boys, S. F.; Bernardi, F. *Mol. Phys.* **1970**, *19*, 553.

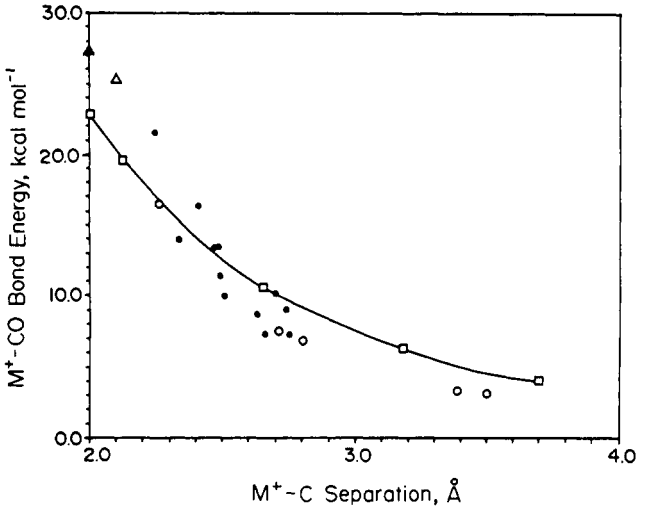

Figure 1. The calculated dissociation energy of several metal carbonyl compounds (MCO^+) versus the metal-to-carbon bond length. Points labeled (●) represent data presented here; (○) from ref 7; (▲) from ref 9; (△) from ref 8. The solid line represents the electrostatic potential, from eq 2.

symbols in the second column of Table I are reported, because all our calculations were done under the restrictions of C_{2v} symmetry (Z or a_1 is the molecular axis, with X and Y being b_1 and b_2, respectively).

Two observations are pertinent from the numerical data of Table I. (a) The M–C bond lengths are very long, ranging from 2.25 Å ($CrCO^+$, $^4\Pi$) to 3.38 Å ($ScCO^+$, $^3\Sigma^+$). For the neutrals, the M–C bond lengths range from 1.67 Å (NiCO, $^1\Sigma^+$) to 1.98 Å (CuCO). In addition, M–C bond lengths for all ground states become progressively smaller as we move from Sc^+ to Cr^+, or from left to right in the periodic table, correlating loosely with atomic radii of the (neutral) metals. Indeed, considering the GVB equilibrium bond lengths we obtain the following differences between MCO^+ bond lengths: 0.11 Å (Sc–Ti), 0.14 Å (Ti–V), and 0.01 Å (V–Cr). These numbers compare favorably with atomic radii differences between the corresponding (neutral) metal atoms: 0.15, 0.13, 0.04 Å. (b) Rather small interaction energies, D_e, are calculated. The binding energies of the states are plotted in Figure 1 versus R_{M-C}; also included are data for the $^1\Sigma^+$, $^1\Delta$, and $^1\Pi$ singlet states[7] of $ScCO^+$, $NiCO^+$ ($^2\Sigma^+$),[8] and $CuCO^+$ ($^1\Sigma^+$)[9] as well as $LiCO^+$ ($^1\Sigma^+$)[22] and Cl_2ScHCO.[23] The curve plotted in Figure 1 is the D_e which is predicted using a purely electrostatic interaction. When looking at this plot, two points should be considered. First, the accuracy of the electrostatic model decreases as one goes to smaller bond lengths. This is because we are keeping terms through $1/R^4$ in the model calculations of the interaction energy, and the neglected higher order terms become more important at smaller values of R. Secondly, the accurate electrostatic interaction energy should always be greater than the ab initio calculated D_e. Note that for the first few points in Figure 1 the calculated electrostatic energy is less than the ab initio bond energy. This is because the omitted terms in the multipolar expansion are most important for these small separations. When the Pauli repulsion becomes important, it increases faster than the electrostatic attraction, resulting in the observed minimum and requiring that the electrostatic term give an upper bound to the binding energy. The agreement with the ab initio calculations is striking and suggests that the electrostatic contribution to the D_e is dominant.

Detailed Results

$ScCO^+$. The valence electronic configuration of Sc^+ is $3d^14s^1$ and gives rise to the ground-state ^3D term. As the CO molecule approaches Sc^+, with its carbon end in a colinear way, three molecular states are possible according to whether the 3d electron

(22) Mavridis, A.; Harrison, J. F., unpublished results.
(23) Rappe, A. K. *J. Am. Chem. Soc.* **1987**, *109*, 5605.

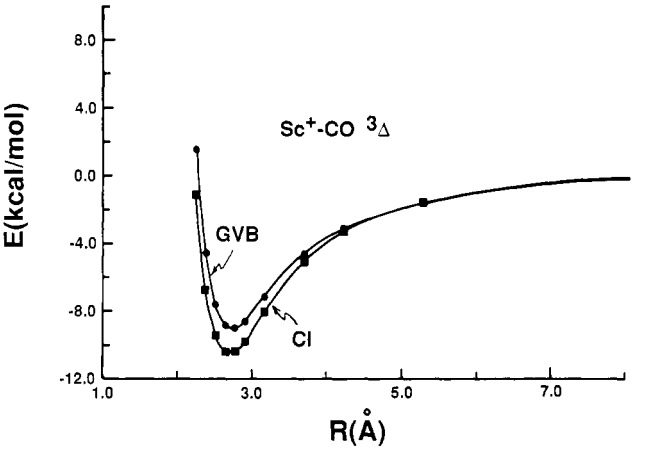

Figure 2. Comparison of the GVB and CI potential energy curves for the $^3\Delta$ state of the $ScCO^+$.

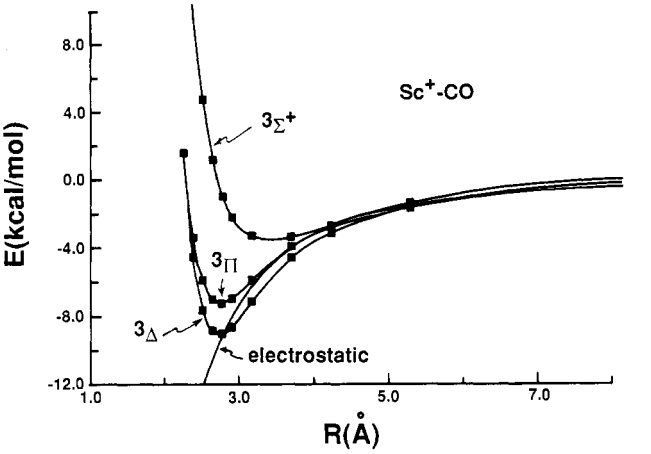

Figure 3. Comparison of the GVB and electrostatic interaction potential energy curves for the $^3\Delta$, $^3\Pi$, and $^3\Sigma^+$ states of $ScCO^+$.

is in a d_σ ($^3\Sigma^+$), d_π ($^3\Pi$), or d_Δ ($^3\Delta$) orbital. The asymptotic GVB wave functions with $i = j = 1$ is given by eq 1 with the two electrons triplet-coupled. Figure 2 shows the GVB potential curves as well as the CI potential curve for the $^3\Delta$ ground state of $ScCO^+$. According to a Mulliken population analysis,[18,19] 0.11, 0.11, and 0.03 *extra* electrons are associated with Sc^+ in the states $^3\Delta$, $^3\Pi$, and $^3\Sigma^+$, respectively (at the equilibrium geometry). Note that in the $^3\Delta$ state back-donation is forbidden by symmetry. At equilibrium the incoming lone pair of CO interacts repulsively with the 4s electron of the metal, and the orbital population is depleted by ~0.05 e. These 0.05 e and the 0.10 e due to ligand-to-metal σ-donation are equally distributed between the empty d_σ and $4p_\sigma$ orbitals of the metal. Exactly the same situation prevails in the $^3\Pi$ state of the system. In the $^3\Sigma^+$ state the charge density along the internuclear axis prevents the close approach of the CO, the lone pair of the latter interacting repulsively with the d_σ electron density. This is reflected in a very long equilibrium Sc–C bond distance (3.380 Å) and the concomitant small interaction energy (3.4 kcal mol^{-1}).

If μ, Θ, and Ω are the dipole, quadrupole, and octapole moment tensor elements along the internuclear axis of CO, relative to its center of mass, and α is the corresponding dipole polarizability, the interaction energy between a +1 point charge and CO in a linear configuration is given by

$$\Delta E = -\mu/R^2 + \Theta/R^3 - \Omega/R^4 - \alpha/2R^4 \qquad (2)$$

with R being the distance between the center of mass of CO and the metal atom. Using μ = +0.04885 au, Θ = −1.6019 au, Ω = +3.9577 au, and α = 16.06 au, all values having been calculated from the CO GVB (4/8) wave function, we obtain ΔE as a function of the Sc–C distance. The results of this electrostatic calculation are shown in Figure 3. The ab initio electrostatic

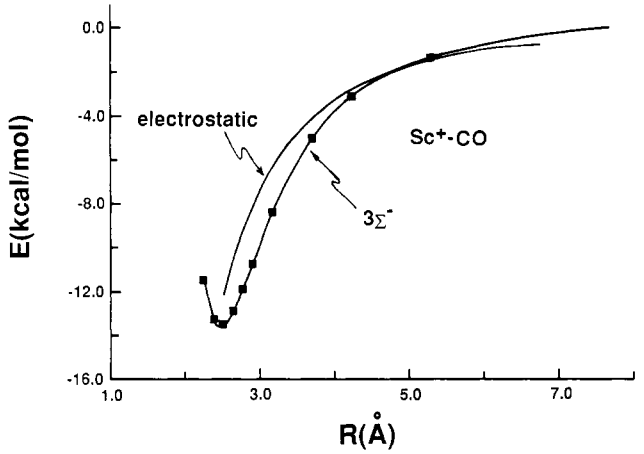

Figure 4. Comparison of the GVB and electrostatic interaction potential energy curves for the $^3\Sigma^-$ state of $ScCO^+$.

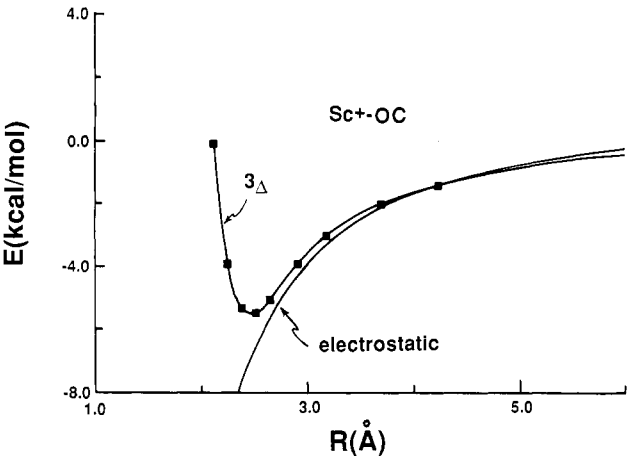

Figure 5. Comparison of the GVB and electrostatic interaction potential energy curves for the $^3\Delta$ state of $ScOC^+$.

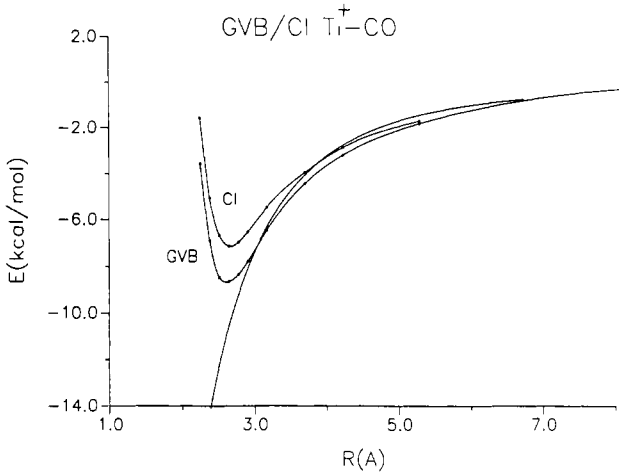

Figure 6. Comparison of the GVB, CI and electrostatic interaction potential energy curves for the $^4\Sigma^-$ state of $TiCO^+$.

expression (eq 2) tracks the "incoming" interaction energy satisfactorily, suggesting that the dominant long-range interaction between Sc^+ and CO is electrostatic in nature, and that the bond energies and equilibrium M^+–CO bond lengths reflect that point at which the electrostatic interaction gives way to the Pauli repulsion developed between the Sc^+ 4s3d electrons and the CO lone pair. As the bond lengths and D_e's of Table I show, this apparently happens first when the 3d electron is in the $3d_\sigma$ orbital ($^3\Sigma^+$), second for the $3d_\pi$ ($^3\Pi$), and last for the $3d_\Delta$ orbital ($^3\Delta$) consistent with their spatial extension along the internuclear axis. As mentioned, the D_e's follow the order $^3\Delta > {}^3\Pi > {}^3\Sigma^+$.

Distributing the two active electrons in Sc^+ as $d\pi^1_{zx}d\pi^1_{zy}$, a mixture of the ^3F and ^3P electronic terms of the metal is obtained. At the SCF level we calculate a splitting $\Delta E(^3F \leftarrow {}^3D) = 0.906$ eV,[24] in contrast to the experimental value of 0.594 eV.[25] The resulting electronic state of $ScCO^+$, with the in situ metal in a ^3F state, has $^3\Sigma^-$ symmetry. The potential energy curve at the GVB level is shown in Figure 4. With the active electrons of Sc^+ being distributed in orbitals that lie "perpendicular" to the internuclear axis, the incoming CO can approach closer to the metal ion, and this in turn is reflected in a larger D_e value. Note that the $^3\Sigma^-$ state is unbound with respect to the ground state by 8 kcal mol^{-1}. The electrostatic expansion (eq 2) represents the interaction fairly well at large internuclear distances but not as well at short distances, owing to the interpenetation of the electron clouds of the two fragments at small separations. The population analysis of the wave function for $ScCO^+$ predicts an additional ~0.06 e on Sc^+. These electrons are transferred to the empty 4s orbital on the metal, with essentially no back-donation to the ligand.

To extend our GVB (4/8) calculations we constructed the SCF+1+2 wave function for the $^3\Delta$ state of $ScCO^+$ using the GVB orbitals. While the absolute energies dropped by 81 kcal mol^{-1} (Table I), the interaction energy (Figure 2) remained practically unchanged compared with that obtained using the GVB description.

The GVB (4/8) and electrostatic interaction energy of Sc^+ with the oxygen end of CO is shown in Figure 5 for the $^3\Delta$ state. The electrostatic interaction once again tracks the ab initio results quite well.

$TiCO^+$. The GVB wave function of $TiCO^+$ is described by eq 1 with $i = 1, j = 2$, the three active electrons of Ti^+ coupled into a quartet state. The ground state[25] of Ti^+ is ^4F and is obtained from the electron distribution $4s^13d^1{}_\Delta 3d^1{}_\sigma$, which in turn leads to a $^4\Delta$ (or a $^4A_1$ state in C_{2v} symmetry) in the molecular environment. Assuming that, in the ground state, the two d electrons are allocated in a perpendicular fashion along the internuclear (Z) axis of the molecule, away from the incoming lone pair of CO, the constructed GVB wave function is of $^4\Sigma^-$ ($^4A_2$) symmetry. Therefore, the in situ metal with configuration $4s^1d\pi^1{}_x d\pi^1{}_y$ is a mixture of ^4F and ^4P states, asymptotically described as $2/\sqrt{5}|^4F\rangle - 1/\sqrt{5}|^4P\rangle$. In Figure 6 we plot the potential energy as a function of Ti^+–C distance. The electrostatic description (eq 2), using the same parameters for the free CO as before, adequately represents the interaction energy. The Mulliken population analysis indicates that 0.13 e are transferred to the metal atom from the CO ligand. As in the $^3\Delta$, $^3\Pi$ states of $ScCO^+$, the repulsive interaction of the CO lone pair with the 4s electron drives ~0.04 e out of the latter orbital; the ~0.17 e are equally distributed between the empty d_σ and $4p_\sigma$ orbitals of the metal. No back-donation is observed. Although a CI calculation, (SCF+1+2) using the GVB orbitals substantially lowers the absolute energy (Table I), and increases the Ti–C bond length by 0.03 Å, the electrostatic interaction description (Figure 6) is essentially unchanged. The destabilization of the molecule by ~1.5 kcal mol^{-1} with respect to the GVB description is associated with the larger bond length as expected. Interestingly, the excited ^4F state of Ti^+ corresponding to the $3d^3$ configuration (which is only 2.5 kcal/mol above the ground ^4F (sd^2)) has an equilibrium Ti–C separation of 2.498 Å and is 0.3 mhartree lower in energy than the sd^2 state. This is consistent with a larger electrostatic interaction permitted by the more compact charge distribution in the d^3 state. Note that in 1974 Mortola and Goddard[26] reported a minimum basis set calculation on the $^4\Sigma^-$ state of $TiCO^+$ in which they assumed a Ti–C bond

(24) Mavridis, A.; Alvarado-Swaisgood, A. E.; Harrison, J. F. *J. Phys. Chem.* **1986**, *90*, 2584.

(25) Moore, C. E. *Atomic Energy Levels*; National Bureau of Standards: Washington, DC, 1971; Vol. I, II.

(26) Mortola, A. P.; Goddard, W. A., III, *J. Am. Chem. Soc.* **1974**, *96*, 1.

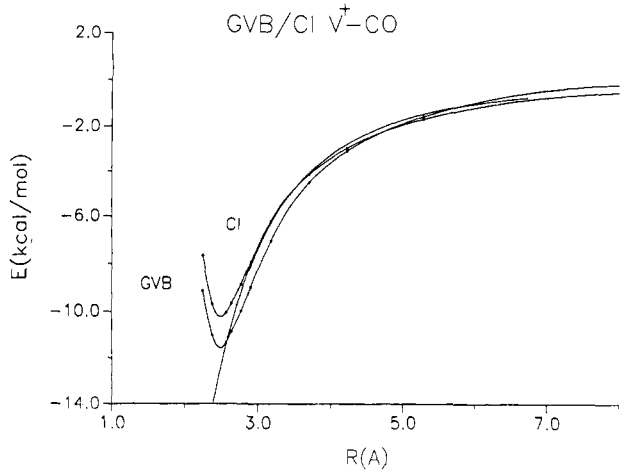

Figure 7. Comparison of the GVB, CI, and electrostatic interaction potential energy curves for $^5\Delta$ state of VCO^+.

length of 1.96 Å. In contrast to our conclusions, these authors find that the CO bonds to the Ti^+ via a σ-donating, π-accepting mechanism. We suspect the Mortola and Goddard calculation suffers from a basis set superposition error.

VCO^+. The electronic ground-state configuration of the V^+ ion is d^4 giving rise to a ^5D ground state.[25] The first excited state is a ^5F ($3d^34s^1$), 0.337 eV above the ^5D. The SCF representation of V^+ inverts the experimental ordering resulting in a ^5F state that is 0.251 eV lower than the ^5D state.[24] The GVB asymptotic wave function is given by (1) with $i = 1, j = 3$ coupled into a quintet spin state. More specifically, the ground state of VCO^+ should be a quintet with the d^3 electrons distributed away from the incoming lone pair on CO. Therefore, the active electronic space on V^+ should have the configuration $4s^1d\pi^1_x d\pi^1_y d^1_\Delta$ which leads to a $^5\Delta$ molecular state (computed as $^5A_1$ under C_{2v} symmetry). Figure 7 shows the potential curves as a function of the V–C separation for both the GVB and CI calculations, as well as the electrostatic potential curve. The latter tracks the interaction energy between V^+ and CO well. The Mulliken population analysis assigns 0.14 additional electron to V^+. At equilibrium the repulsive Pauli interaction between the lone pair on the C of CO and the $4s^1$ electron on the metal atom depletes the latter by ~0.11 e. Of the 0.25 e (0.14 + 0.11), 0.16 and 0.09 flow into the empty d_σ and $4p_\sigma$ orbitals of the metal, respectively; no d_π back-donation is observed. Table I shows that the CI calculation leads to a slightly larger V–C bond length with an accompanying decrease of the binding energy by 1.4 kcal mol^{-1}. Note that the CI separates to the d^4 configuration even though the orbitals used were for the sd^3 configuration of V^+. The CI description is sufficiently flexible to overcome the shortcomings in the d^4 description due to the sd^3 orbitals, and results in the correct ordering of the states of V^+. Although not explicitly considered, we expect that the $3d^2_\pi 3d^2_\delta$ configuration will have an energy comparable to that of the $^5\Delta$ state and may even be a mhartree or so lower. One does not expect a large difference since the spatial extension of the charge distribution in the $\pi^2\delta^2$ configuration is similar to that in the $\sigma\pi^2\delta$ configuration.

$CrCO^+$. When CO approaches Cr^+ in its ^6S ground state[25] colinearly, the resultant molecular electronic state is of $^6\Sigma^+$ symmetry. The interaction energy calculated with the GVB wave function (eq 1, $i = 0, j = 5$) is shown in Figure 8. Also plotted in Figure 8 is the potential curve of $^3\Sigma^-$ state for $ScCO^+$. The resemblance is remarkable and suggests that the mechanism which leads to binding in both molecules is the same and, largely, electrostatic. The population analysis indicates that ~0.06 e has transferred from the ligand to the metal ion, exactly the same as in the $^3\Sigma^-$ state of $ScCO^+$. Very little charge (~0.02 e) flows into the empty 4s orbital of Cr^+, while the rest goes into the $4p_\sigma$. There is no d_π back-donation at all. By moving a d_σ electron of Cr^+ to a $3d_\pi$ orbital the configuration $3d\sigma^0 3d\pi^2_x 3d\pi^1_y 3d^1_{\Delta+} 3d^1_{\Delta-}$ is obtained which leads to a $^4\Pi$ state ($^4B_1$ under C_{2v} symmetry)

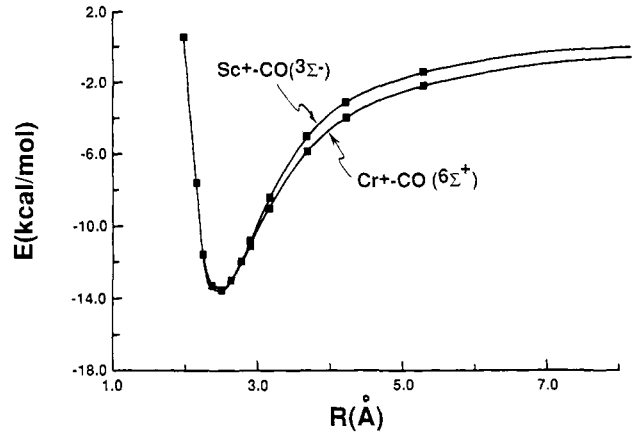

Figure 8. Comparison of the GVB interaction energies for the $CrCO^+$ ($^6\Sigma^+$) and $ScCO^+$ ($^3\Sigma^-$) molecules.

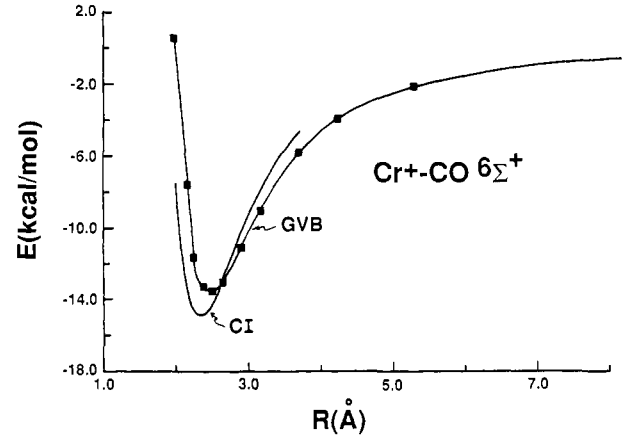

Figure 9. Comparison of the GVB and CI interaction energies for the $^6\Sigma^+$ state of $CrCO^+$.

in the molecular environment. Our GVB results indicate that, upon this excitation of Cr^+, the Cr–C bond length is reduced to 2.250 Å and the bond strength is increased to 21.5 kcal mol^{-1}. The increase in bond energy observed on promotion of the d_σ electron of Cr^+ appears to reflect the fact that the excitation allows Cr^+ and CO to move closer to each other, increasing the electrostatic interaction.

Figure 9 also compares the GVB results with CI results (SCF+1+2) constructed using the GVB orbitals) for the $^6\Sigma^+$ state of $CrCO^+$. Although the differential energy effect is insignificant, the CI predicts a shorter Cr–C bond length. A possible explanation of the bond-length shortening is that at the GVB level the in situ Cr^+ is always described at the SCF level and therefore the five parallel spins in the ^6S state of Cr^+ are overcorrelated, producing an "inflated" atom which is then mitigated at the CI level.

Conclusions

The binding mechanism of a single CO ligand to the early transition metal +1 ions, Sc^+, Ti^+, V^+, and Cr^+, is totally different from the traditional Dewar–Chatt view. While the latter view appears to have some validity for the neutral species,[5,6,8,9] our findings strongly suggest that the fundamental binding component, for the metal cations, is electrostatic in nature, with no more than 10% σ ligand-to-metal donation and practically no metal-to-ligand d_π back-donation. Our results are consistent with those of Bauschlicher[8] ($NiCO^+$) and Merchan et al.[9] ($CuCO^+$). The evidence presented here supporting dominance of electrostatic interaction is as follows.

(a) M–C bond lengths are large relative to similar neutral species as evidenced from Table I.

(b) The binding energies, D_e, depend only on the bond length and the attractive component of the $M–CO^+$ potential curves and are well represented by the (ab initio) electrostatic formula using

the calculated electrostatic properties of free CO. In Figure 1 we have also included $LiCO^+$ ($^1\Sigma^+$)[22] and Cl_2ScHCO.[23] In $LiCO^+$ the binding clearly is electrostatic, with no opportunity for back-donation. The possibility of σ donation is also very remote. In Cl_2ScHCO the Cl substituents remove electrons from Sc giving it considerable Sc^+ character. The calculated[23] ScCO bond length and bond energy (2.406 Å and 16.4 kcal/mol) are consistent with those calculated for the transition metal monocarbonyl cations.

(c) The Mulliken population analysis results indicate that very little charge transfer takes place. Notwithstanding the well-known pitfalls of the method,[20] the trends are rather clear.

The question naturally arises as to why the bonding is totally different between MCO and MCO^+? The σ-d_π view is a synergistic one: the σ ligand donation assists the d_π back-donation and vice versa. If the one cannot take place, the effect of the other is also greatly diminished. For the ionic systems the d_π metal back-donation does not occur mainly for energetic reasons. Electron transfer out of the M^+ ion is prohibitively costly in light of the values of the second IE of the metals. The second IE's for Sc^+, Ti^+, V^+, and Cr^+ are 12.9, 13.6, 14.2, and 16.5 eV, respectively, as opposed to ~6.7 eV on the average for the first IE of the metal atoms. The gain in energy due to covalent binding, if charge is transferred from M^+ to CO, cannot compensate for the cost of that transfer and therefore the electrostatic interaction dominates.

Acknowledgment. This work was partially supported under NSF Grants CHE8519752 (J.F.H.) and CHE 8722111 (J.A.).

Registry No. Sc^+, 14336-93-7; Ti^+, 14067-04-0; V^+, 14782-33-3; Cr^+, 14067-03-9.

Stereochemical Studies on Protonated Bridgehead Amines. ^{1}H NMR Determination of Cis and Trans B–C Ring-Fused Structures for Salts of Hexahydropyrrolo[2,1-*a*]isoquinolines and Related C Ring Homologues. Capture of Unstable Ring-Fused Structures in the Solid State†

Bruce E. Maryanoff,*,‡ David F. McComsey,‡ Ruth R. Inners,‡ Martin S. Mutter,‡ Gary P. Wooden,§ Stephen L. Mayo,§ and R. A. Olofson§

Contribution from the Chemical Research Department, McNeil Pharmaceutical, Spring House, Pennsylvania 19477, and Department of Chemistry, The Pennsylvania State University, University Park, Pennsylvania 16802. *Received January 11, 1988*

Abstract: Acid-addition salts of tricyclic isoquinolines **2a/b**, **3a/b**, **4a–4c**, **5**, **6a/b**, **7**, **8a/b**, **9a/b**, and **17a/b** were studied by high-field ^{1}H NMR in $CDCl_3$ solution. Cis (e.g., **14** and **15** in Figure 1) and trans (e.g., **13**) B–C ring-fused structures were identified by using the vicinal ^3J(CH–NH) coupling constants, which demonstrate a Karplus-like behavior. In some cases, we initially observed a trans form, which converted to a cis A form by NH proton exchange. For **4c**·HBr, the exchange process was slowed by addition of trifluoroacetic acid. In many cases, cis A and cis B structures were preferred in solution. The pendant phenyl group exerted a strong influence on the preferred solution structure. Observation of the initial, unstable trans-fused structures was related to their capture in the solid state and release intact on dissolution. X-ray diffraction was performed on the HBr salts of **2a** (B–C cis), **2b** (B–C cis), and **4c** (B–C trans). The result for **4c**·HBr confirmed the connection between the initial trans form in solution and the solid state. For **17b**·HCl two conformers, associated with hindered rotation about the bond connecting the 2,6-disubstituted phenyl group to the tricyclic array, were detected at ambient probe temperature; however, rotamers were not observed for either of the two forms (trans and cis A) of **17a**·HBr. Two conformers were also found for **16b**·HBr. Temperature-dependent behavior was recorded in the ^{1}H NMR spectra of **17b**·HBr and **16b**·HBr; the activation free energy for interconversion of conformers was estimated to be in the vicinity of 17 kcal/mol for the former and 14–15 kcal/mol for the latter. The ^{1}H NMR spectrum of butaclamol hydrochloride (**20**·HCl), a potent neuroleptic agent, in Me_2SO-d_6 revealed two species in a ratio of 81:19, which were assigned as trans and cis A forms, respectively. ^{1}H NMR data for various free bases are also presented and discussed. Empirical force field calculations on three model hydrocarbons are discussed from a perspective of finding an explanation for the configurational/conformational behavior of the bridgehead ammonium salts. Diverse literature examples of structures for protonated bridgehead amines are also discussed. A tentative rationale is suggested for the preference of cis A forms in some protonated tetrahydroisoquinoline derivatives.

Although substantial information has been acquired on the structural and conformational properties of alicyclic amines with nitrogen at the bridgehead position, such as bicyclic [*m.n.*0] compounds where *m* and *n* = 3 or 4, the corresponding protonated species (i.e., acid-addition salts) have been largely ignored.[1] Since this type of molecular framework is part and parcel of a wide variety of alkaloid structures,[2] as well as several biologically active compounds,[2-5] further study of acid-addition salts would be useful.

* Current address of correspondence author: Chemical Research Department, Janssen Research Foundation, Spring House, PA 19477. (JRF is a new entity in Johnson & Johnson from reorganization of the Pharmaceutical Sector.)

† This paper was presented in part in the "Symposium on Heterocyclic Chemistry" at the 18th Middle Atlantic Regional Meeting of the American Chemical Society, Newark, NJ, May 1984; paper ORGN-246. It was also presented at the 194th National Meeting of the American Chemical Society, New Orleans, LA, Sept 1987; paper ORGN-122.

‡ McNeil Pharmaceutical.

§ The Pennsylvania State University.

(1) (a) Eliel, E. L.; Allinger, N. L.; Angyal, S. J.; Morrison, G. A. *Conformational Analysis*; Wiley: New York, 1965. (b) Skvortsov, I. M. *Russ. Chem. Rev.* **1979**, *48*, 1979. (c) Crabb, T. A.; Newton, R. F.; Jackson, D. *Chem. Rev.* **1971**, *71*, 109. (d) Crabb, T. A.; Katritsky, A. R. *Adv. Heterocycl. Chem.* **1984**, *36*, 1.

(2) (a) Dalton, D. R. *The Alkaloids: The Fundamental Chemistry—A Biogenetic Approach*; Marcel Dekker: New York, 1979. (b) Cordell, G. A. *Introduction to Alkaloids: A Biogenetic Approach*; Wiley: New York, 1981. (c) Glasby, J. S. *Encyclopedia of the Alkaloids*; Plenum: New York, 1975; Vol. 1 and 2.

0002-7863/89/1511-2487$01.50/0